© 2014. Published by The Company of Biologists Ltd | Journal of Cell Science (2014) 127, 1911–1923 doi:10.1242/jcs.138982

RESEARCH ARTICLE

Insulin elicits a ROS-activated and an IP_3-dependent Ca^{2+} release, which both impinge on GLUT4 translocation

Ariel Contreras-Ferrat[1,2], Paola Llanos[1,2], César Vásquez[1], Alejandra Espinosa[3], César Osorio-Fuentealba[1], Manuel Arias-Calderon[1], Sergio Lavandero[1], Amira Klip[4], Cecilia Hidalgo[1,5] and Enrique Jaimovich[1,*]

ABSTRACT

Insulin signaling includes generation of low levels of H_2O_2; however, its origin and contribution to insulin-stimulated glucose transport are unknown. We tested the impact of H_2O_2 on insulin-dependent glucose transport and GLUT4 translocation in skeletal muscle cells. H_2O_2 increased the translocation of GLUT4 with an exofacial Myc-epitope tag between the first and second transmembrane domains (GLUT4myc), an effect additive to that of insulin. The anti-oxidants *N*-acetyl L-cysteine and Trolox, the $p47^{phox}$–NOX2 NADPH oxidase inhibitory peptide gp91-ds-tat or $p47^{phox}$ knockdown each reduced insulin-dependent GLUT4myc translocation. Importantly, gp91-ds-tat suppressed insulin-dependent H_2O_2 production. A ryanodine receptor (RyR) channel agonist stimulated GLUT4myc translocation and insulin stimulated RyR1-mediated Ca^{2+} release by promoting RyR1 *S*-glutathionylation. This pathway acts in parallel to insulin-mediated stimulation of inositol-1,4,5-trisphosphate (IP_3)-activated Ca^{2+} channels, in response to activation of phosphatidylinositol 3-kinase and its downstream target phospholipase C, resulting in Ca^{2+} transfer to the mitochondria. An inhibitor of IP_3 receptors, Xestospongin B, reduced both insulin-dependent IP_3 production and GLUT4myc translocation. We propose that, in addition to the canonical α,β phosphatidylinositol 3-kinase to Akt pathway, insulin engages both RyR-mediated Ca^{2+} release and IP_3-receptor-mediated mitochondrial Ca^{2+} uptake, and that these signals jointly stimulate glucose uptake.

KEY WORDS: Skeletal muscle, NOX2, RyR1, Ca^{2+} transient, Inositol 1,4,5-trisphosphate, Metabolic control

INTRODUCTION

Reactive oxygen species (ROS) are relevant second messengers in physiological and pathological cellular processes ranging from the immune response to cell growth and differentiation (Bashan et al., 2009; Horie et al., 2008; Paulsen and Carroll, 2010). Cellular ROS include singlet oxygen, superoxide anion, hydrogen peroxide (H_2O_2), the hydroxyl radical and other partially reduced oxygen derivatives. H_2O_2 is the most suitable to act as a second messenger because of its high specificity, stability and regulation (Forman et al., 2010). In particular, insulin-dependent H_2O_2 production contributes to Akt activation and glucose uptake in 3T3-L1 adipocytes (Mahadev et al., 2001).

The ROS-generating NOX2 enzyme is a multi-protein complex formed by three cytoplasmic subunits ($p47^{phox}$, $p67^{phox}$ and $p40^{phox}$), a G protein (Rac1 or Rac2), and two membrane-bound subunits ($p22^{phox}$ and NOX2, formerly known as $gp91^{phox}$) (Bedard and Krause, 2007). Adult muscle fibers express NOX2 (Javeshghani et al., 2002) in transverse tubules (T-tubules) (Hidalgo et al., 2006), suggesting that in this tissue NOX2-mediated ROS generation and the ensuing redox effects might be highly localized. We have previously shown that NOX2 generates ROS in skeletal muscle myotubes in response to insulin (Espinosa et al., 2009). A rise in cellular ROS promotes redox modifications of skeletal muscle proteins (Hidalgo et al., 2004) and a global 'phosphatase tone' (Wright et al., 2009) in both skeletal and cardiac muscle. The thiol (-SH) group of cysteine residues undergoes covalent reactions with oxidants, which produce modifications, such as *S*-glutathionylation, that give rise to functional alterations. Several intracellular ROS target proteins relate to muscle excitation–contraction coupling (Barreiro and Hussain, 2010). In particular, the open probability of ryanodine receptor type 1 (RyR1) increases upon H_2O_2-dependent oxidation (Donoso et al., 2000; Hidalgo and Donoso, 2008).

In striated muscle cells, two Ca^{2+} channels, the inositol-1,4,5-triphosphate (IP_3) receptor (IP3R) and RyR1, mediate intracellular Ca^{2+} release from the sarcoplasmic reticulum (SR). The IP3R channels respond to IP_3 generation by phospholipase C (PLC), producing cytoplasmic Ca^{2+} signals related to metabolism (Pacher et al., 2008) and gene expression (Jaimovich and Carrasco, 2002; Liberona et al., 2008). The RyR1 channels, which release Ca^{2+} in response to plasma membrane depolarization, contribute to the characteristic excitation–contraction coupling process of skeletal muscle cells (Protasi et al., 2002). A recent report proposes that RyR1 channels, by controlling passive Ca^{2+}efflux from the SR to the cytoplasm, represent key factors in the management of the resting muscle cytoplasmic Ca^{2+}concentration (Eltit et al., 2010).

Interestingly, our groups have reported that: (1) insulin elevates intracellular Ca^{2+} levels via NOX2 activation in primary neonatal myotubes (Espinosa et al., 2009), (2) NOX2-dependent ROS production promotes RyR1 *S*-glutathionylation and stimulates RyR1-mediated Ca^{2+} release from triad-enriched vesicles isolated from adult skeletal muscle (Hidalgo et al., 2006), and (3) intracellular Ca^{2+} contributes to the insulin-dependent increase in glucose uptake in cardiomyocytes (Contreras-Ferrat et al., 2010). The physiological mechanism whereby insulin activates NOX2, however, remains unknown.

[1]Centro de estudios Moleculares de la Célula, Facultad de Medicina; Facultad de Ciencias Químicas y Farmacéuticas, Universidad de Chile, Santiago, Chile. [2]Instituto de Investigación en Ciencias Odontológicas, Facultad de Odontología, Universidad de Chile, Santiago, Chile. [3]Escuela de Tecnología Médica, Facultad de Medicina, Universidad de Chile, Avenido Libertador Bernardo O'Higgins 1058, Santiago, Chile. [4]The Hospital for Sick Children, Toronto, ON M5G 1X8, Canada. [5]Biomedical Neuroscience Institute and Programa de Fisiología y Biofísica, Instituto de Ciencias Biomédicas, Facultad de Medicina, Universidad de Chile, Avenida Independencia 1027, Independencia, Santiago, Chile.

*Author for correspondence (ejaimovi@med.uchile.cl)

Received 1 August 2013; Accepted 31 January 2014

Journal of Cell Science (2014) 127, 1911–1923 doi:10.1242/jcs.138982

An insulin-dependent Ca^{2+} increase, detected with the Ca^{2+} fluorescent dye Indo-1, occurs near the plasma membrane in single muscle fibers isolated from the *Flexor digitorum brevis* (FDB) muscle (Bruton et al., 1999), and this has been associated with insulin-stimulated Ca^{2+} influx via L-type voltage-dependent Ca^{2+} channels (Cav1.1). In cultured myotubes from rat skeletal muscle, insulin induces RyR1-mediated Ca^{2+} transients measured with the fluorescent Ca^{2+} indicator Fluo3 (Espinosa et al., 2004). In skeletal muscle fibers, 2-aminoethoxydiphenyl borate (2-APB) inhibits both basal and insulin-dependent Ca^{2+} influx (Lanner et al., 2006). A contribution of intracellular Ca^{2+} stores to glucose uptake was proposed on the basis that dantrolene, an inhibitor of the interaction between Cav1.1 and RyR1 that inhibits depolarization-induced Ca^{2+} release (Bannister, 2013), prevents insulin-dependent glucose uptake in adipocytes (Li et al., 2006). In those cells, decreasing intracellular Ca^{2+} signals decreased insulin-stimulated glucose uptake and Akt phosphorylation (Whitehead et al., 2001). In skeletal muscle fibers, Ca^{2+} influx is important for full stimulation of glucose uptake (Lanner et al., 2009; Lanner et al., 2006).

Notably, it remains unknown how insulin elicits intracellular Ca^{2+} signals and what are the sources of these signals. Given the prominence of insulin action in skeletal muscle, unraveling this mechanism is paramount to understand the regulation of glucose uptake by this hormone.

RESULTS

ROS induce GLUT4myc translocation and glucose uptake in skeletal muscle myotubes

We used L6-GLUT4myc myotubes (myotubes expressing GLUT4 with an exofacial Myc-epitope tag between the first and second transmembrane domains) to investigate the effect of ROS on glucose uptake. L6-GLUT4myc myotubes stimulated with insulin displayed an increase in exofacial exposure of the Myc epitope (Fig. 1A), as previously reported (Ishikura and Klip, 2008). L6-GLUT4myc myotubes stimulated for 20 min with different concentrations of H_2O_2 displayed a concentration-dependent increase of GLUT4myc translocation to the cell surface; as little as 0.01 mM H_2O_2 produced a stimulatory effect, which reached its maximum at 0.1 mM H_2O_2; treatment with 1 mM H_2O_2 did not produce an extra increase (Fig. 1A). The effects of 0.1 mM H_2O_2 were additive to those of insulin (Fig. 1B); of note, insulin-dependent GLUT4myc translocation to the cell surface was prevented by 1 mM H_2O_2, indicating a biphasic, concentration-dependent role of ROS as enhancers or inhibitors of insulin signaling.

To evaluate whether the increase in surface GLUT4myc reflects an increase in glucose uptake, we used the conventional pulse and chase activity assay using [^{3}H]-2-deoxy glucose. A low concentration of H_2O_2 (0.1 mM) boosted insulin-dependent glucose uptake, whereas a higher H_2O_2 concentration (1 mM) prevented this response (Fig. 1C). To study the possible participation of ROS in insulin-dependent glucose uptake, we pre-incubated L6-GLUT4myc myotubes with two types of widely used antioxidant agents: *N*-acetylcysteine (NAC) or Trolox, a water-soluble vitamin E derivative. Interestingly, both antioxidant agents partially inhibited the stimulation of GLUT4myc surface exposure produced by insulin in myotubes (Fig. 1D) but not in myoblasts, in which insulin effectively stimulated GLUT4myc translocation (data not shown). These results suggest that ROS-dependent stimulation of GLUT4myc surface exposure requires a more mature state of differentiation.

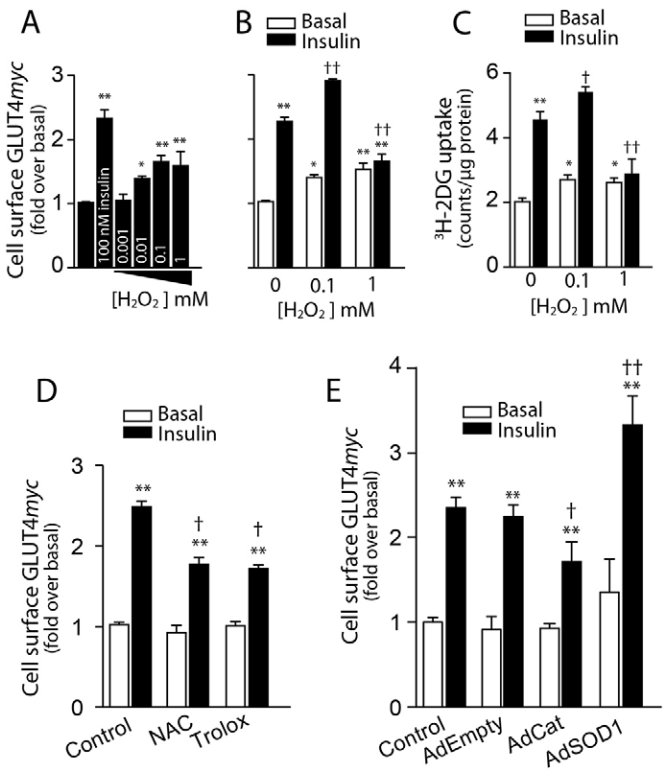

Fig. 1. Dual effects of H_2O_2 on insulin-dependent GLUT4 translocation to the cell surface. (A) Cell surface GLUT4myc was evaluated in myotubes incubated for 20 min with 100 nM insulin or with the indicated concentration of H_2O_2. (B) Myotubes were co-stimulated with 100 nM insulin and H_2O_2 (100 μM or 1 mM) for 20 min before measuring GLUT4myc content at the cell surface. (C) Myotubes were co-stimulated with 100 nM insulin and H_2O_2 (100 μM or 1 mM) for 20 min before measuring the chase of ^{3}H-2DG for 10 min. (D) Cell surface GLUT4myc content was evaluated in myotubes pre-incubated for 30 min with 5 mM NAC or 10 mM Trolox, and subsequently stimulated for 20 min with 100 nM insulin in the presence of each antioxidant agent. (E) Myotubes were transduced 48 h before measuring cell surface GLUT4myc content with empty adenovirus or with adenoviruses containing catalase (AdCat) or superoxide dismutase (AdSOD1) (MOI=10,000). Values are mean±s.d. $^*P<0.01$, $^{**}P<0.001$ compared with basal; $^{\dagger}P<0.01$, $^{\dagger\dagger}P<0.001$ compared with insulin-stimulated cells (one-way ANOVA followed by Tukey post-hoc test).

In order to establish causality using molecular tools, we tested the participation of cytoplasmic antioxidant enzymes on insulin-induced GLUT4myc translocation to the cell surface. To this aim, L6-GLUT4myc myotubes were transduced with adenoviruses encoding superoxide dismutase 1 (AdSOD1) or the wild-type form of catalase (AdCat). Superoxide dismutase (SOD1) produces H_2O_2 from superoxide species, increasing the available basal levels of H_2O_2, whereas catalase rapidly induces H_2O_2 dismutation reducing its effective half-life. Transduced myotubes displayed *in vitro* enzyme activities over 15-fold higher compared to non-transduced cells (data not shown). Myotubes overexpressing SOD1 displayed a bigger increase in GLUT4myc translocation in response to insulin; in contrast, myotubes overexpressing catalase displayed reduced insulin-induced stimulation of GLUT4myc translocation to the cell surface (Fig. 1E). These results suggest a role for oxidative signaling in GLUT4myc translocation and glucose uptake downstream of insulin stimulation in L6-GLUT4myc skeletal myotubes.

Journal of Cell Science (2014) 127, 1911–1923 doi:10.1242/jcs.138982

Insulin increases cytoplasmic H_2O_2 production through PKC-dependent NOX2 activation, which promotes GLUT4myc translocation to the cell surface

As shown in Fig. 1, H_2O_2 induced an increase in both GLUT4myc translocation and glucose uptake; the molecular entities involved in these responses are unknown, as is the mechanism responsible for ROS generation downstream of insulin signaling in skeletal muscle cells. To determine whether insulin enhances cytoplasmic H_2O_2 production, we transiently transfected L6-GLUT4myc myotubes with a plasmid vector encoding the molecular H_2O_2 biosensor HyPer targeted to the cytoplasm (HyPer-cyto). Recording in real time revealed that Hyper-cyto effectively sensed low H_2O_2 concentrations in L6-GLUT4myc myotubes (Fig. 2A); addition of vehicle did not change the basal fluorescence levels (Fig. 2A). Addition of insulin induced a fast and transient increase in HyPer-cyto fluorescence emission, which reached a maximum at 7±3 s post stimuli and took 143±32 s to decay thereafter (mean±s.d.; Fig. 2B, black trace).

NOX2 is a protein complex canonically activated by translocation of $p47^{phox}$, $p67^{phox}$ and the small GTP-binding protein Rac1 to the plasma membrane, where they form the active enzyme by interacting with the membrane integral proteins gp91 and p22 (Maghzal et al., 2012). Indirect immunofluorescence determinations showed $p47^{phox}$ subunits located in the cytoplasm of myotubes, showing poor expression in myoblasts (data not shown). To explore NOX2 participation in insulin-induced H_2O_2 generation, we inhibited NOX2 with the specific peptide gp91-ds-tat (Wei et al., 2008), which contains the $gp91^{phox}$ sequence linked to the HIV tat peptide. L6-GLUT4myc myotubes

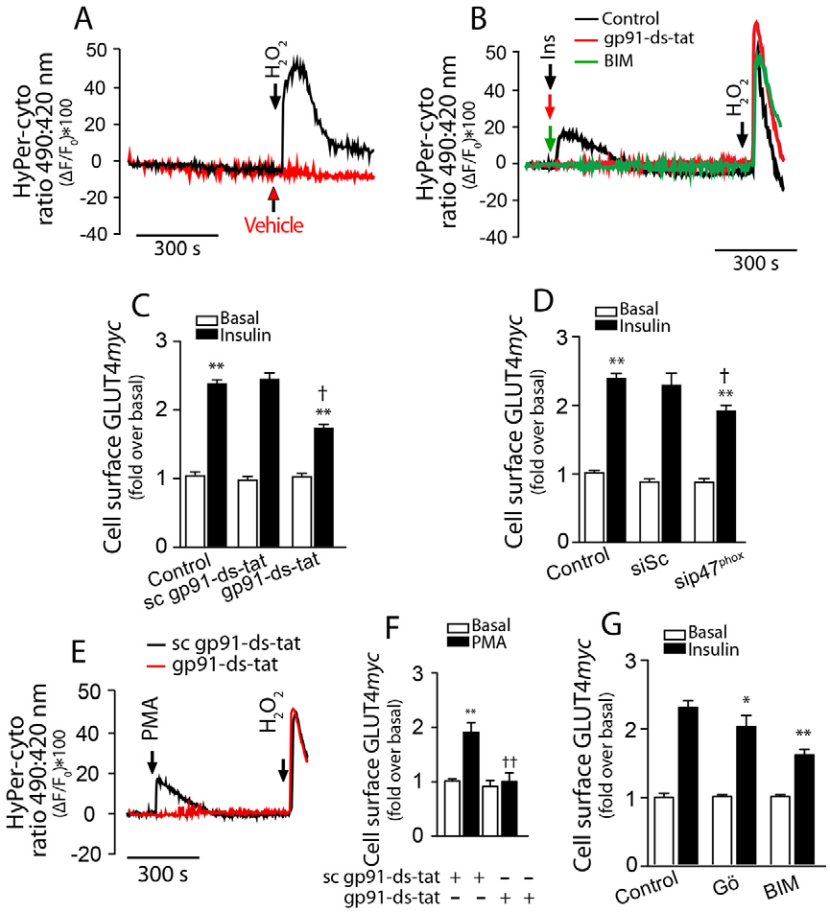

Fig. 2. Insulin-induced H_2O_2 production promotes GLUT4myc translocation through PKC-dependent NOX2 activation. (A) Myotubes transfected with the cytoplasmic H_2O_2 sensor HyPer-cyto were treated with 100 μM H_2O_2 (black trace) or with vehicle (red trace). (B) Addition of 100 nM insulin increased the HyPer-cyto fluorescence ratio (black trace); treatment with 5 μM gp91-ds-tat (NOX2 inhibitory peptide, green trace) or pre-treatment with 1 μM of BIM (conventional and novel PKC inhibitor, red trace) abrogated the increase of the HyPer-cyto fluorescence ratio induced by 100 nM insulin. The results correspond to the fluorescence ratio 490 nm:420 nm. (C) The effects of adding 100 nM insulin on cell surface GLUT4myc translocation were tested in control myotubes or in myotubes pre-incubated for 30 min with 5 μM gp91-ds-tat or 5 μM scrambled (sc) gp91-ds-tat (inactive peptide). (D) Effects of 100 nM insulin on cell surface GLUT4myc translocation were tested in control myotubes or in myotubes transfected with 50 nM p47phox siRNA ($sip47^{phox}$) or 50 nM control siRNA (siSc). Myotubes transfected for 4 h with each siRNA were maintained for 48 h before adding 100 nM insulin; GLUT4myc translocation was measured 20 min after insulin addition. (E) Myotubes transfected with the HyPer-cyto sensor and pre-incubated for 30 min with 5 μM gp91-ds-tat or 5 μM sc gp91-ds-tat as indicated were stimulated with 1 μM PMA (phorbol ester). As a control, 1 mM H_2O_2 was added at the end of the experiment. (F) Myotubes were stimulated with 1 μM PMA for 20 min and surface GLUT4myc was evaluated in myotubes pre-incubated for 30 min with 5 μM gp91-ds-tat or 5 μM sc gp91-ds-tat. (G) L6-GLUT4myc myotubes were pre-incubated with 1 μM Gö6976 (conventional PKC inhibitor) or 1 μM BIM (conventional and novel PKC inhibitor) during the 30 min before insulin addition. In C, D, F and G, results are mean±s.d. Statistical analysis was performed with one-way ANOVA followed by Tukey post-hoc test. *P<0.01, **P<0.001 compared with basal; †P<0.01, ††P<0.001 compared with insulin-stimulated cells (one-way ANOVA followed by Tukey post-hoc test).

Journal of Cell Science (2014) 127, 1911–1923 doi:10.1242/jcs.138982

pre-incubated for 1 h with gp91-ds-tat or its inactive scrambled sequence sc-gp91-ds-tat were stimulated with insulin. Incubation with the inhibitory peptide abolished insulin-dependent H_2O_2 production (Fig. 2B, red trace), whereas the inactive peptide did not inhibit this response (data not shown). In order to explore whether protein kinase C (PKC) contributes to NOX2 activation, L6-GLUT4myc myotubes were pre-incubated with 1 μM bisindolylmaleimide (BIM), a conventional inhibitor of PKCα and PKCβ, also described to inhibit PKCδ. This PKC inhibitor completely suppressed insulin-dependent H_2O_2 production (Fig. 2B, green trace). Moreover, addition of 5 mM NAC drastically reduced basal HyPer-cyto fluorescence and prevented insulin-induced H_2O_2 production; NAC also moderately lowered the fluorescent signal induced by addition of 100 μM H_2O_2, used as positive control (data not shown). These combined results strongly suggest that NOX2 mediates insulin-dependent ROS generation through PKC activation.

To elucidate whether NOX2 contributes to insulin-dependent GLUT4myc translocation, we inhibited NOX2 with gp91-ds-tat. To this aim, L6-GLUT4myc myotubes were pre-incubated for 1 h with gp91-ds-tat or its inactive scrambled sequence sc-gp91-ds-tat and were stimulated with insulin for 20 min in the presence of these synthetic peptides. Pre-incubation with the gp91-ds-tat peptide partially reduced insulin-dependent GLUT4myc translocation; in contrast, transfection with the scrambled sequence did not affect this response (Fig. 2C). Furthermore, the pharmacological NOX2 inhibitors apocynin or diphenyliodonium (DPI) reduced but did not fully suppress insulin-dependent GLUT4myc translocation to the cell surface (supplementary material Fig. S1A). Myotubes transiently transfected with siRNA (50 nM) against the regulatory NOX2 subunit $p47^{phox}$ displayed significantly reduced $p47^{phox}$ levels (supplementary material Fig. S1C) and lower GLUT4myc translocation following insulin addition than either control myotubes or myotubes transfected with a scrambled siRNA (Fig. 2D).

Different PKC enzymes contribute to insulin signaling

Previous studies indicate that a diacylglycerol-mimicking phorbol ester (Wright et al., 2004) and compounds that increase intracellular Ca^{2+} (Wright et al., 2005) stimulate glucose uptake in cultured cells and isolated rodent muscles. In muscle cells, it has been suggested that activation of PKCζ and PKCλ increases GLUT4 translocation, although this finding has been somewhat controversial (Liu et al., 2006; Powell et al., 2003; Stretton et al., 2010). Moreover, PKCα and PKCβ promotes $p47^{phox}$ activation and plasma membrane translocation to assemble the NOX2 activated complex in macrophages (San José et al., 2009). It has been widely accepted that phosphorylation via PKC activates NOX2 in many systems. To test whether direct PKC activation promotes NOX2-dependent H_2O_2 production, we stimulated myotubes with the phorbol ester 12-myristate 13-acetate (PMA, a universal activator of classical and novel PKCs). In L6-GLUT4myc myotubes, PMA induced a fast and transient increase in HyPer-cyto fluorescence, which reached a maximum value 3±2 s post stimuli (Fig. 2E), with a decay half time of 126±41 s (mean±s.d.; presumably reflecting the breakage kinetics of the H_2O_2-induced HyPer-cyto disulfide bridge by cellular reducing systems). Pre-incubation of myotubes with gp91-ds-tat but not with the inactive peptide abolished PMA-dependent H_2O_2 production (Fig. 2E). Furthermore, incubation of myotubes with PMA for 20 min strongly increased GLUT4myc translocation to the cell surface; the synthetic inhibitory peptide gp91-ds-tat abolished this increase (Fig. 2F). Co-stimulation of myotubes with PMA and insulin resulted in a significant extra increase in exofacial exposure of the Myc epitope over that produced by insulin alone (supplementary material Fig. S1B). Both the PKC inhibitor Gö6976 (specific for Ca^{2+}-dependent PKCs) and more so BIM (a general inhibitor of types α, β, γ and δ PKCs), significantly reduced GLUT4 translocation induced by insulin (Fig. 2G). Taken together, these results suggest that PKC is involved in the increased NOX2-mediated cytoplasmic H_2O_2 generation and GLUT4myc translocation stimulated by insulin.

Exofacial exposure of GLUT4myc induced by insulin requires RyR1-mediated Ca^{2+} release

L6-GLUT4myc myotubes pre-incubated with the Ca^{2+} dye indicator Fluo4 am were mounted in a chamber and intracellular Ca^{2+} levels were recorded frame-by-frame in a confocal microscope. After 1 min recording, we replaced the Ca^{2+}-containing resting solution with a Ca^{2+}-free solution (Fig. 3A–C, blue dashed lines). Addition of 100 μM H_2O_2 produced a rapid increase in intracellular Ca^{2+} levels that did not occur in cells pre-treated with 50 μM ryanodine, strongly suggesting that ROS induced RyR1-mediated Ca^{2+} release (Fig. 3A). Insulin addition in Ca^{2+}-free resting medium generated whole-cell Ca^{2+} transients, which were not present in cells pre-incubated with 50 μM ryanodine for 3 h or 5 μM gp91-ds-tat for 30 min (Fig. 3B). Addition of the Ca^{2+} ionophore ionomycin to cells kept in Ca^{2+}-free solution induced a rapid rise in fluorescence in all conditions, presumably by inducing Ca^{2+} release from intracellular stores (Fig. 3A,B). To induce RyR1-mediated Ca^{2+} release, we used the specific RyR agonist 4-chloro-m-cresol (4-CMC). In Ca^{2+}-free resting medium, 4-CMC induced a fast increase in intracellular Ca^{2+}, which slowly decreased to near basal levels after 5 min (Fig. 3C); ionomycin addition was used as a positive control at the end of the recording.

4-CMC also induced an increase in GLUT4myc translocation to the cell surface, and this effect was more evident in insulin co-stimulated myotubes (Fig. 3D). Translocation of GLUT4myc induced by 4-CMC was completely inhibited in myotubes pre-incubated with inhibitory doses of ryanodine (data not shown). Moreover, insulin-dependent GLUT4myc translocation was also significantly lower in myotubes pre-incubated with ryanodine (Fig. 3D), whereas myotubes pre-incubated jointly with the NOX2 gp91-ds-tat inhibitor and ryanodine did not show additional inhibition over that produced by ryanodine alone (Fig. 3D). We used ionomycin to determine whether an increase in intracellular Ca^{2+} levels stimulates GLUT4myc translocation to the cell surface. Myotubes stimulated with 1 μM ionomycin for 5 min showed increased exofacial exposure of the Myc epitope that was additive to the stimulation induced by insulin (Fig. 3E). Insulin-dependent GLUT4myc translocation did not occur in L6-GLUT4myc myotubes pre-incubated with BAPTA-AM for 30 min; this intracellular Ca^{2+} chelator did not affect the basal levels of translocation (Fig. 3E). This strategy was complemented by overexpressing the parvalbumin Ca^{2+} buffer protein fused to DsRed, as the cell tracker (PV–DsRed). A plasmid encoding only DsRed was used as control. Cells were fixed in non-permeabilized conditions and the exofacial exposure of the Myc epitope was assayed in single cells. PV–DsRed-expressing cells were unresponsive to insulin and exhibited decreased basal exposure of the Myc epitope (Fig. 3F). Moreover, non-transfected myotubes showed a notable increase in the amount of insulin-induced cell

Journal of Cell Science (2014) 127, 1911–1923 doi:10.1242/jcs.138982

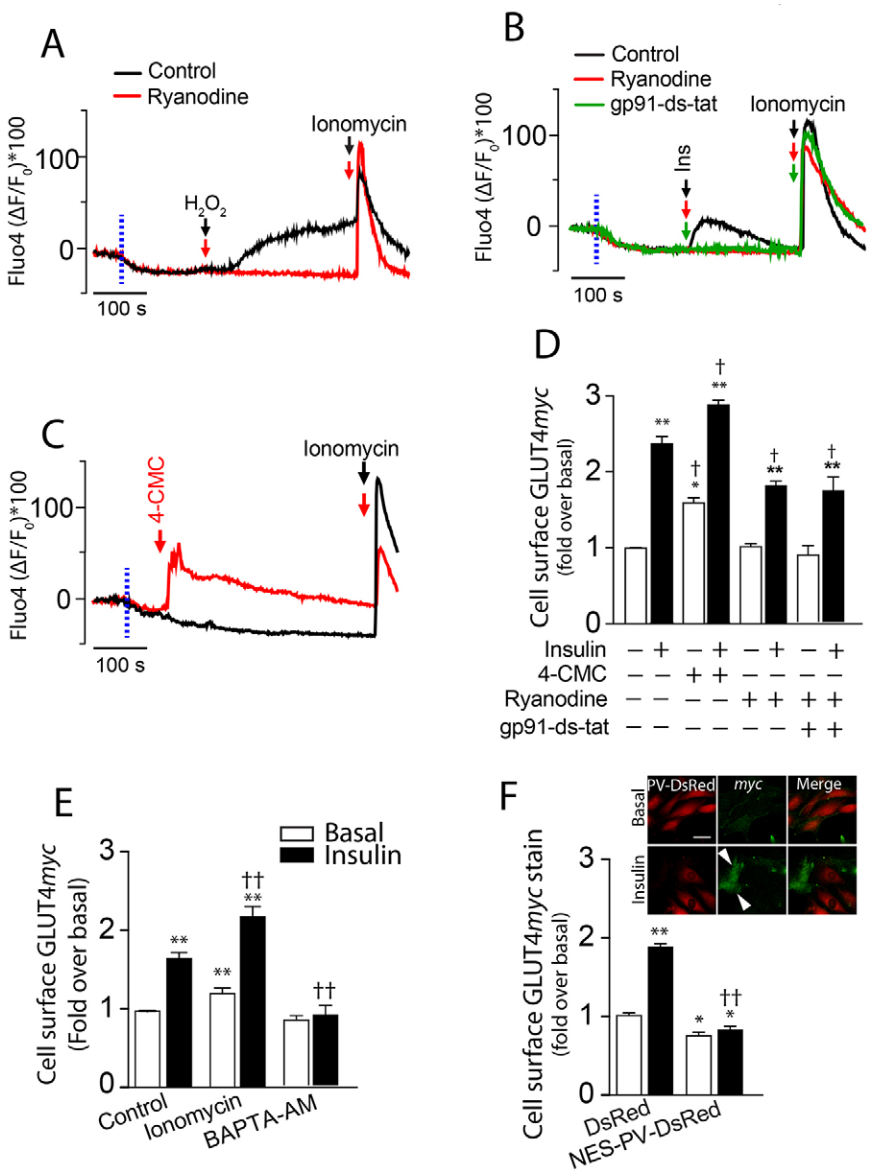

Fig. 3. Insulin-dependent translocation of GLUT4myc to the cell surface requires RyR1-mediated intracellular Ca^{2+} increase. (A) Control myotubes (black trace) or myotubes pre-incubated for 3 h with 50 μM ryanodine (RyR inhibitor, red trace) were incubated for 30 min with 5.4 μM Fluo4 am before addition of 100 μM H_2O_2, as indicated by the arrows. (B) Control myotubes (black trace), myotubes pre-incubated for 3 h with 50 μM ryanodine (red trace) or myotubes pre-incubated for 30 min with 5 μM gp91-ds-tat (NOX2 inhibitory peptide, green trace) were incubated for 30 min with 5.4 μM Fluo4 am in the presence of the respective compound before addition of 100 nM insulin at the arrows. (C) Myotubes were incubated for 30 min with 5.4 μM Fluo4 am before addition (at the arrow) of 500 μM 4-CMC (specific RyR agonist, red trace); control (black trace). Ca^{2+} transients depicted in A, B and C were recorded in Ca^{2+}-free medium, the addition of which is indicated by the dashed blue line. At the end of the recording period, 1 μM ionomycin (Ca^{2+} ionophore) was added as a positive control. (D) GLUT4myc translocation was assayed in controls or after addition of 500 μM 4-CMC (RyR agonist), 100 nM insulin or both. Myotubes were pre-incubated for 3 h with 50 μM ryanodine (RyR inhibitor) or with 50 μM ryanodine for 3 h and 5 μM gp91-ds-tat, during the last 30 min. (E) GLUT4myc translocation was assayed in control myotubes before or 5 min after addition of 100 nM insulin, 1 μM ionomycin (Ca^{2+} ionophore) or both. In parallel experiments, GLUT4myc translocation was assayed in myotubes pre-incubated for 30 min with 50 μM BAPTA-AM (intracellular Ca^{2+} chelator), before or 5 min after addition of 100 nM insulin. (F) L6-GLUT4myc cells were transiently transfected with parvalbumin fused to DsRed (PV–DsRed) and surface Myc epitope levels were detected in non-permeabilized control single cells (empty bars) or in single cells stimulated with 100 nM insulin for 20 min (solid bars). Cells transfected with DsRed were used as control. The image in the inset shows a representative experiment. Values are mean±s.d. $^{*}P<0.01$, $^{**}P<0.001$ compared with basal; $^{\dagger}P<0.01$, $^{\dagger\dagger}P<0.001$ compared with insulin-stimulated cells (one-way ANOVA followed by Tukey post-hoc test).

surface GLUT4myc stain (Fig. 3F, arrowheads). These combined experiments suggest that the cytoplasmic Ca^{2+} increase produced by stimulation of Ca^{2+} release through ROS-mediated RyR1 activation forms part of the insulin signaling pathways that promote GLUT4myc translocation to the cell surface.

Insulin-dependent H_2O_2 production induced RyR1 *S*-glutathionylation in skeletal muscle cells

ROS generation induces reversible *S*-glutathionylation of reactive cysteine residues (Pastore and Piemonte, 2012). To detect whether *S*-glutathionylation of proteins increases in insulin-stimulated cells, myotubes were stimulated with insulin or H_2O_2 for 1 min and the indirect co-immunofluorescence against *S*-glutathionylated protein adducts or RyR1 was detected with specific antibodies. In basal conditions, myotubes showed very low fluorescence when tested with the antibody against *S*-glutathionylated protein adducts, indicating low basal levels of this redox modification (Fig. 4A). In contrast, myotubes stimulated with 100 μM H_2O_2 exhibited significantly higher *S*-glutathionylated protein levels, which partially overlapped with RyR1 immunofluorescence yielding a Pearson coefficient of 0.44±0.06 and Mander's coefficients M1 and M2 of 0.68±0.09 and 0.61±0.09 (mean±s.d.), respectively (Fig. 4A). Of note, 1 min exposure to 100 nM insulin increased *S*-glutathionylated protein adducts with a clear overlap with the RyR1 stain, reaching a Pearson coefficient of 0.782±0.07 and Mander's coefficients M1 and M2 of 0.92±0.07 and 0.91±0.02, respectively (Fig. 4A). As the resolution provided by co-immunofluorescence experiments cannot ascertain the actual RyR1 *S*-glutathionylation levels, we used a novel high-resolution technique that yields positive results for molecules located less than 40 nm apart. Specific RyR1 *S*-glutathionylation was ascertained using *in situ* proximity ligation assay (PLA) probes, which detect closely positioned antibodies with an optimal distance of 20–30 nm (Söderberg et al., 2006). To this aim, cultured myotubes stimulated with insulin or H_2O_2 for 1 min and rapidly fixed were probed both with anti-RyR1 and anti-*S*-glutathionylated protein adducts; RyR1 *S*-glutathionylation is indicated by the appearance of fluorescent dots (Fig. 4B). The basal levels of RyR1 *S*-glutathionylation were 5±1.4 dots/

Journal of Cell Science (2014) 127, 1911–1923 doi:10.1242/jcs.138982

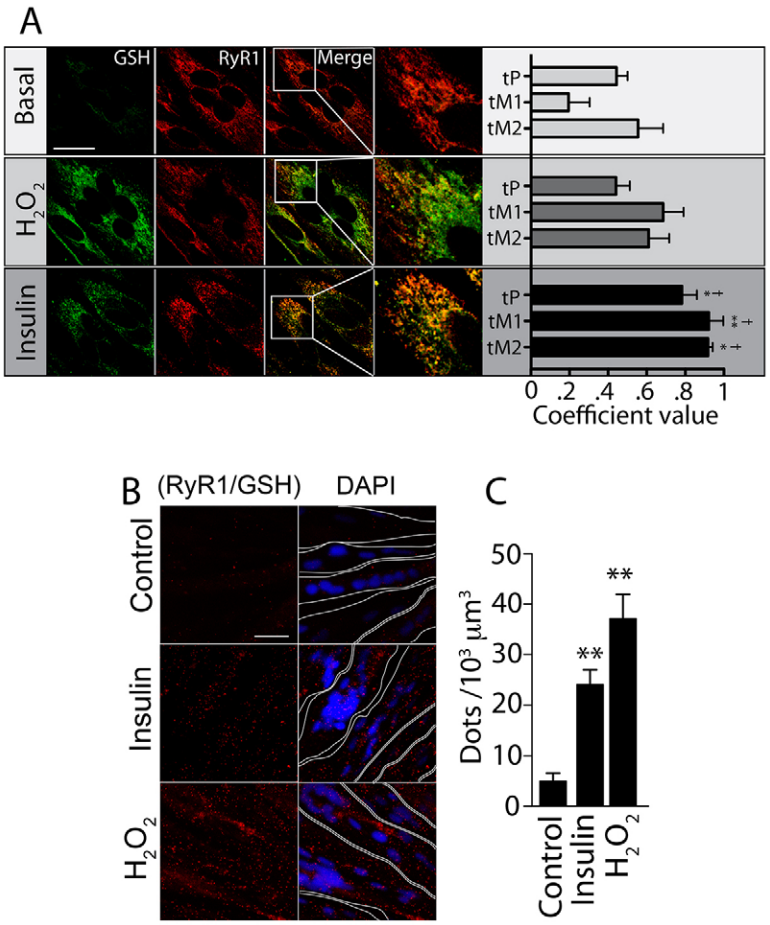

Fig. 4. Insulin enhances RyR1 *S*-glutathionylation in L6-GLUT4myc myotubes. (A) Representative experiment showing co-immunofluorescence images against RyR1 (red) and *S*-glutathionylated protein adducts (green), in myotubes under basal conditions or 1 min after adding 100 µM H_2O_2 or 100 nM insulin. The panels on the right right show the corresponding values of Pearson (tP) and Mander's coefficients (tM1 and tM2). For details, see text. (B) Proximity ligation assay (PLA) probes were used to detect specific RyR1 *S*-glutathionylation (red dots). Representative images taken from control myotubes, or from myotubes incubated for 1 min with 100 nM insulin or 100 µM H_2O_2. (C) The positive red dots, such as those illustrated in B, were counted in all *z*-stack slices and normalized to the total stack volume. In A and C, results are mean±s.d. $*P<0.01$, $**P<0.001$ compared with basal; $^{\dagger}P<0.01$, $^{\dagger\dagger}P<0.001$ compared with insulin-stimulated cells (one-way ANOVA followed by Tukey post-hoc test).

1000 µm^3, whereas in insulin-stimulated myotubes these levels increased to 24±2.5 dots/1000 µm^3. Cells treated with 100 µM H_2O_2 displayed 37±4.2 dots/1000 µm^3 (mean±s.d.; Fig. 4C).

Insulin-dependent exofacial exposure of GLUT4myc and glucose uptake in skeletal myotubes require IP3R activation

IP3R-dependent Ca^{2+} signaling plays a relevant role in cell physiology (Foskett et al., 2007). The IP3R increases its open probability in response to IP_3 produced by PLC activation. We explored whether IP3R-generated Ca^{2+} signals also contribute to insulin-dependent GLUT4myc translocation in L6 and primary rat neonatal myotubes. L6-GLUT4myc myotubes express all three IP3R isoforms (supplementary material Fig. S2A). The IP3R1 isoform displayed a cytoplasmic and nuclear distribution showing diffuse stain with condensed highly fluorescent dots. Interestingly, the IP3R2 isoform presented a striated transversal pattern in the cytoplasm. The IP3R3 isoform displayed poor fluorescence intensity compared to the other isoforms, detected with the same microscope settings (supplementary material Fig. S2A).

Insulin addition produced a fast increase in intracellular IP_3 levels, which increased from the basal values of 12.3±1.6 to 24.8±2.4 pg/mg of protein in 30 s (mean±s.d.; Fig. 5A). Both, LY294002 and U-73122 [broad inhibitors of phosphoinositide 3-kinase (PI3K) and PLC, respectively] inhibited insulin-stimulated IP_3 production, whereas U-73343, an inactive analog of U-73122, did not affect IP_3 production (Fig. 5A). Pre-incubation of myotubes with the PI3K inhibitor LY294002 did not affect the basal myc epitope levels but abolished insulin-dependent GLUT4myc translocation (Fig. 5B). We found that the PLC inhibitor U73122 partially inhibited, whereas the inactive analogue U73343 had no effect on, insulin-dependent GLUT4myc translocation in myotubes (Fig. 5B). The last step in IP_3-dependent Ca^{2+} release is the interaction of IP_3 with the IP_3-binding site of IP3R. Myotubes pre-incubated with Xestospongin B, a specific IP3R inhibitor, displayed a partial reduction of insulin-dependent GLUT4myc translocation (Fig. 5C). Combined treatment with both intracellular Ca^{2+} channels inhibitors, Xestospongin B and ryanodine, strongly inhibited insulin-dependent Myc epitope externalization, which reached values not significantly different from the controls not treated with insulin (Fig. 5C).

To further test the involvement of IP3R2, L6-GLUT4myc myotubes were transfected with siRNA against IP3R2, which produced a >90% reduction in protein levels compared with non transfected cells or with a control non-targeting oligonucleotide (Fig. 5D). Insulin addition to L6-GLUT4myc myotubes transfected with the IP3R2 siRNA produced a lower stimulation of Myc epitope exposure compared to the stimulation produced in control cells or in cells transfected with the control siRNAs (Fig. 5E).

Myotubes overexpressing IP3R2 wild type exhibited increased basal levels of myc epitope exposure compared to control or DsRed-transfected cells, detected by indirect immunofluorescence in non-permeabilized cells (Fig. 5F). Moreover, insulin-stimulated myoblasts overexpressing IP3R2 displayed significantly increased

Journal of Cell Science (2014) 127, 1911–1923 doi:10.1242/jcs.138982

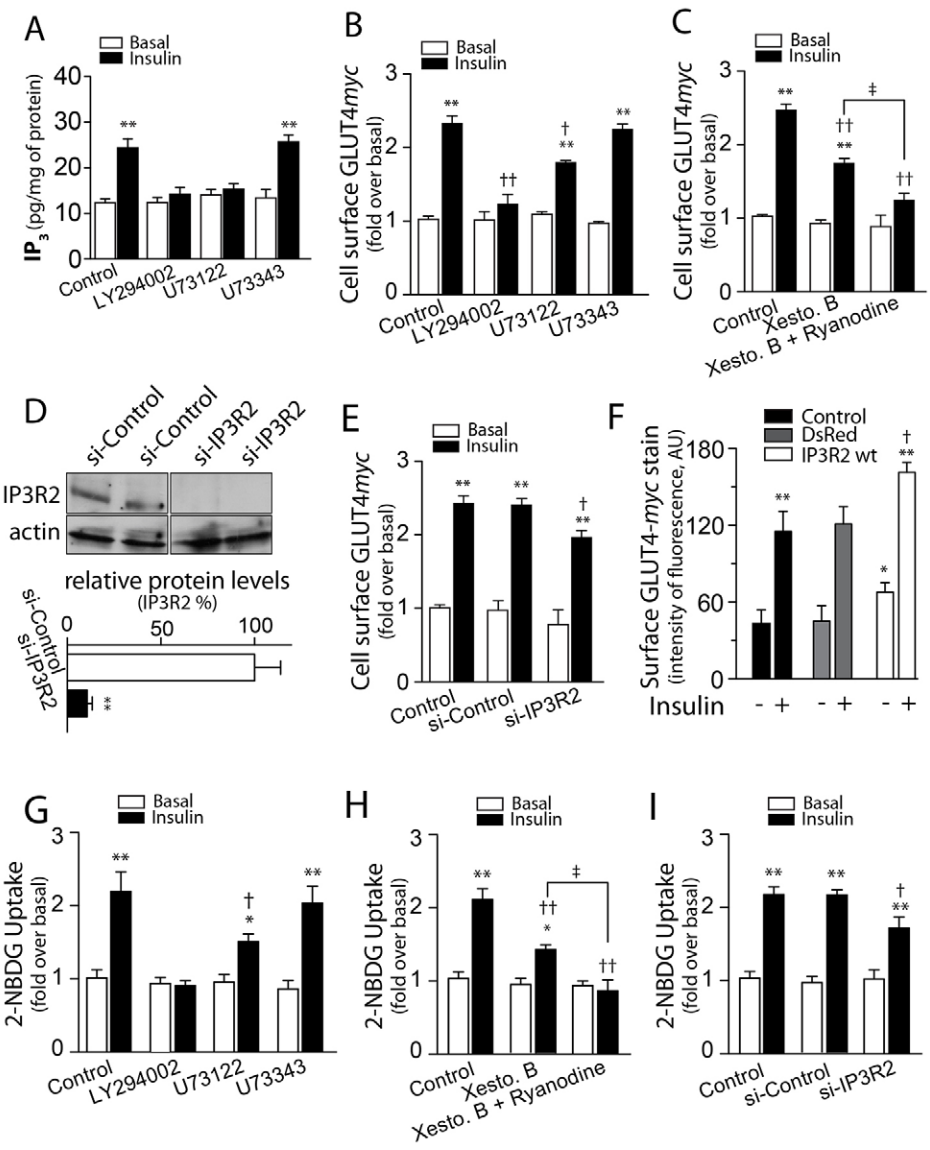

Fig. 5. Insulin-induced GLUT4 translocation to the cell surface engages IP3R. (A) IP_3 mass was evaluated before or 1 min after adding 100 nM insulin to control myotubes or to myotubes pre-incubated for 30 min with 10 μM LY294002 (a PI3K inhibitor), 10 μM U73122 (a PLC inhibitor) or 10 μM U73343 (an inactive U73122 analog). (B) Cell surface GLUT4myc levels were evaluated in myotubes pre-incubated for 30 min with 10 μM LY294002, 10 μM U73122 or 10 μM U73343, before or 20 min after addition of 100 nM insulin. (C) Cell surface GLUT4myc levels were evaluated in control myotubes, in myotubes pre-incubated for 30 min with 5 μM Xestospongin B (specific IP3R inhibitor), or pre-incubated for 3 h with 50 μM ryanodine (RyR inhibitor) plus 5 μM Xestospongin B (Xesto. B) added during the last 30 min. (D) Immunoblot showing IP3R2 protein content in L6-GLUT4myc myotubes transfected with control siRNA (si-Control) or IP3R2 siRNA (si-IP3R2). Lanes correspond to separate samples for each condition. The lower panel shows a quantification of the relative protein level. (E) Cell surface GLUT4myc levels were evaluated in control L6-GLUT4myc myotubes and in myotubes transfected with IP3R2 siRNA or control siRNA, before or 20 min after addition of 100 nM insulin. (F) L6-GLUT4myc cells were transiently co-transfected for 24 h with DsRed and wild-type IP3R2 (IP3R2wt) or with a control construct, and stimulated with 100 nM insulin for 20 min. The Myc epitope was quantified in non-permeabilized cells. (G) 2-NBDG uptake was assayed in control primary neonatal rat myotubes or in myotubes pre-incubated for 30 min with 10 μM LY294002, 10 μM U73122 or 10 μM U7334, before or 20 min after addition of 100 nM insulin. (H) 2-NBDG uptake was assayed before or 20 min after addition of 100 nM insulin in control myotubes or in myotubes pre-incubated for 30 min with 5 μM Xestospongin B or pre-incubated for 3 h with 50 μM ryanodine plus 5 μM Xestospongin B added in the last 30 min. (I) 2-NBDG uptake was assayed in control myotubes or in myotubes transfected for 4 h with 50 nM IP3R2 siRNA or control siRNA and maintained for 48 h before addition of 100 nM insulin. Results are mean±s.d. $*P<0.01$, $**P<0.001$ compared with basal; $^{\dagger}P<0.01$, $^{\dagger\dagger}P<0.001$ compared with insulin-stimulated myotubes; $^{\ddagger}P<0.01$ compared with myotubes treated with Xestospongin B and stimulated with insulin (one-way ANOVA followed by Tukey post-hoc test).

surface GLUT4myc stain compared to control cells or to cells transfected only with DsRed (supplementary material Fig. S2B).

Because it is important to validate these results in skeletal muscle primary cultures, we used the well-characterized myotube preparation from mice neonatal muscle. Insulin addition stimulated glucose transport in primary myotubes by over 2-fold, as determined by measurement of the uptake of the fluorescent glucose analog 2-NBDG (Fig. 5G). LY294002 suppressed and U73122 partially decreased insulin-dependent 2-NBDG uptake, whereas the inactive analog U73343 had no effect (Fig. 5G). Xestospongin B reduced insulin-dependent 2-NBDG uptake, whereas co-incubation with Xestospongin B and

Journal of Cell Science (2014) 127, 1911–1923 doi:10.1242/jcs.138982

ryanodine suppressed this response (Fig. 5H). The stimulatory effect of insulin on 2-NBDG uptake was partially reduced in primary myotubes transfected with siRNA against IP3R2; transfection with the control siRNA did not induce changes (Fig. 5I). These combined results show that IP3R2 has a relevant participation in insulin-dependent GLUT4myc translocation and 2-NBDG uptake in skeletal muscle cells.

Insulin-dependent IP3R activation regulates mitochondrial Ca^{2+} and pH levels in L6-GLUT4myc cells

To investigate whether insulin promotes mitochondrial Ca^{2+} uptake, and hence stimulates mitochondrial function, we used the mitochondrial-targeted ratiometric PeriCaM (mito-PeriCaM) as a Ca^{2+} probe. This probe displays two excitation maxima (410–440 nm and 480–490 nm), each one presenting a maximal emission wavelength of 535 nm (Fonteriz et al., 2010). The 410–440 nm peak displays high Ca^{2+} sensitivity, as decreasing fluorescence emission, whereas the 480–490 nm is highly responsive to $[H^+]$, decreasing fluorescence emission when the pH goes down. Following insulin addition, L6-GLUT4myc myotubes transfected with mito-PeriCaM and mounted 24 h later for viewing under a microscope, displayed fast and transient increases in both mitochondrial Ca^{2+} levels and matrix pH (Fig. 6A). Ca^{2+} levels decreased towards the basal level at 10 min post-stimuli (data not shown). The area under the curve, corresponding to the first 5 min post insulin was measured (Fig. 6B). The serine/threonine kinase Akt inhibitor $Akt_i1/2$ did not affect insulin-dependent mitochondrial Ca^{2+} uptake of L6-GLUT4myc myotubes transiently transfected with mito-PeriCaM, whereas pre-incubation with inhibitory doses of ryanodine for 3 h produced a partial decrease (Fig. 6C). Pre-incubation with Xestospongin B or Ruthenium Red (RuRed) to inhibit the mitochondrial Ca^{2+} uniporter (MCU), or co-transfection with siRNA against IP3R2 significantly reduced insulin-dependent mitochondrial Ca^{2+} uptake (Fig. 6C). To associate the insulin-dependent mitochondrial Ca^{2+} handling to GLUT4myc translocation, myotubes were pre-incubated for 30 min with RuRed or $Akt_i1/2$; both inhibitors reduced insulin-dependent GLUT4myc translocation (Fig. 6D). Interestingly, co-incubation with $Akt_i1/2$ and RuRed, or with $Akt_i1/2$ and Xestospongin B, did not increase the inhibitory effects of RuRed or Xestospongin B alone (Fig. 6D).

To test the participation of PI3K signaling on insulin-dependent mitochondrial Ca^{2+} uptake, primary myotubes were co-transfected with Δp85dn, a dominant-negative form of the PI3K IA regulatory subunit. These cells displayed significantly reduced insulin-dependent mitochondrial Ca^2 uptake (Fig. 6E). Co-transfection of the PH domain of centaurin α1 fused to eGFP [a molecular inhibitor of phosphatidylinositol 3,4,5-trisphosphate (PIP_3) signaling] together with mito-PeriCaM or of an IP_3 sponge corresponding to the IP_3-binding site of IP3R (M49-IP_3 sponge), acting as competitive inhibitors of PIP_3 signaling and IP_3 production respectively, suppressed insulin-dependent mitochondrial Ca^{2+} uptake (Fig. 6E). Co-transfection with a mutated construct without sponge capacity (M30-IP_3 sponge) did not alter the stimulatory effect of insulin (Fig. 6E). Additional experiments to inhibit mitochondrial Ca^{2+} uptake (RuRed) or IP3R function (M49-IP_3 sponge) reduced insulin-dependent 2-NBDG uptake in primary myotubes (Fig. 6F). All these experiments were made in labeled single living cells, as described in the Materials and Methods, in order to avoid dealing with the low transfection efficiency (less than 5%) observed in primary myotubes. These data suggest that the increased mitochondrial Ca^{2+} and pH levels induced by insulin are associated with GLUT4 translocation to the cell surface and glucose uptake in muscle cells.

DISCUSSION

Insulin binding to its receptor on muscle cells promotes tyrosine phosphorylation of insulin receptor substrate-1, inducing PI3K activation, which in turn activates the serine/threonine kinase Akt and the small G protein Rac1 to mobilize translocation of GLUT4 to the muscle membrane (Zaid et al., 2008). For years, reports have proposed that additional input occurs from discrete and possibly localized changes in H_2O_2 and cytoplasmic Ca^{2+} concentration, as well as from PLC-derived signals, but the origin and precise mode of action of these putative mediators has remained elusive. Here, we show how these two signals originate, and that they arise in parallel and jointly contribute to insulin-induced GLUT4 translocation in skeletal myotubes. Specifically, we report that insulin leads to activation of NOX2-dependent H_2O_2 production to promote RyR1 *S*-glutathionylation and RyR1-mediated Ca^{2+} release; in parallel, there is sequential activation of PI3K and PLC resulting in IP_3 generation and activation of IP3R-mediated Ca^{2+} release, which promotes mitochondrial Ca^{2+} uptake. Collectively, these two signaling modes contribute to the net gain in surface GLUT4 levels elicited by insulin. We propose a new integrative mechanism of insulin signaling that comprises RyR1 Ca^{2+} channel redox modifications and ligand-dependent IP3R activation in skeletal muscle cells (Fig. 7).

The ROS–RyR1 branch

As for many actions of ROS, the impact of H_2O_2 on insulin action and on glucose transport in particular is biphasic (Mahadev et al., 2001; Rudich et al., 1998; Bashan et al., 2009). Using a battery of molecular and pharmacological tools, we show that insulin promotes NOX2-dependent H_2O_2 generation. Furthermore, we show that exogenous H_2O_2, induces, at all concentrations, the translocation of the GLUT4 transporter to the surface of myotubes, and also either potentiates or decreases, respectively, the effects of insulin in myotubes co-stimulated with low or high H_2O_2 concentrations. These evidences suggest that Ca^{2+} release mediates the stimulatory effect of H_2O_2 on insulin action, but the inhibitory effect of high doses of H_2O_2 on insulin action likely implies an additional mechanism. A previous report has shown that mice lacking glutathione peroxidase 1 ($Gpx^{-/-}$), a key enzyme for physiological ROS removal, and fed a high-fat diet are protected from insulin resistance; their increased insulin sensitivity correlates with enhanced oxidation of the protein tyrosine phosphatase PTEN and is reversed by NAC (Loh et al., 2009). Consistent with those findings, we report that chemical (NAC, Trolox) and molecular (AdCat) antioxidants decrease insulin-dependent GLUT4 translocation in L6-GLUT4myc myotubes, whereas the potentiated effect displayed by myotubes overexpressing SOD1 presumably relates to a high pro-oxidative state. In neonatal cardiac myocytes, acute H_2O_2 increases cytoplasmic Ca^{2+} levels and GLUT4 translocation to the cell surface (Horie et al., 2008). A role of Ca^{2+}/calmodulin-dependent protein kinase kinase (CaMKK) in H_2O_2-dependent ERK1/2 and Akt activation has also been reported in smooth muscle cells (Bouallegue et al., 2009).

Chronic exposure of adipocytes to H_2O_2 reduces IRS1-asociated PI3K activity and impairs insulin-stimulated GLUT4

Journal of Cell Science (2014) 127, 1911–1923 doi:10.1242/jcs.138982

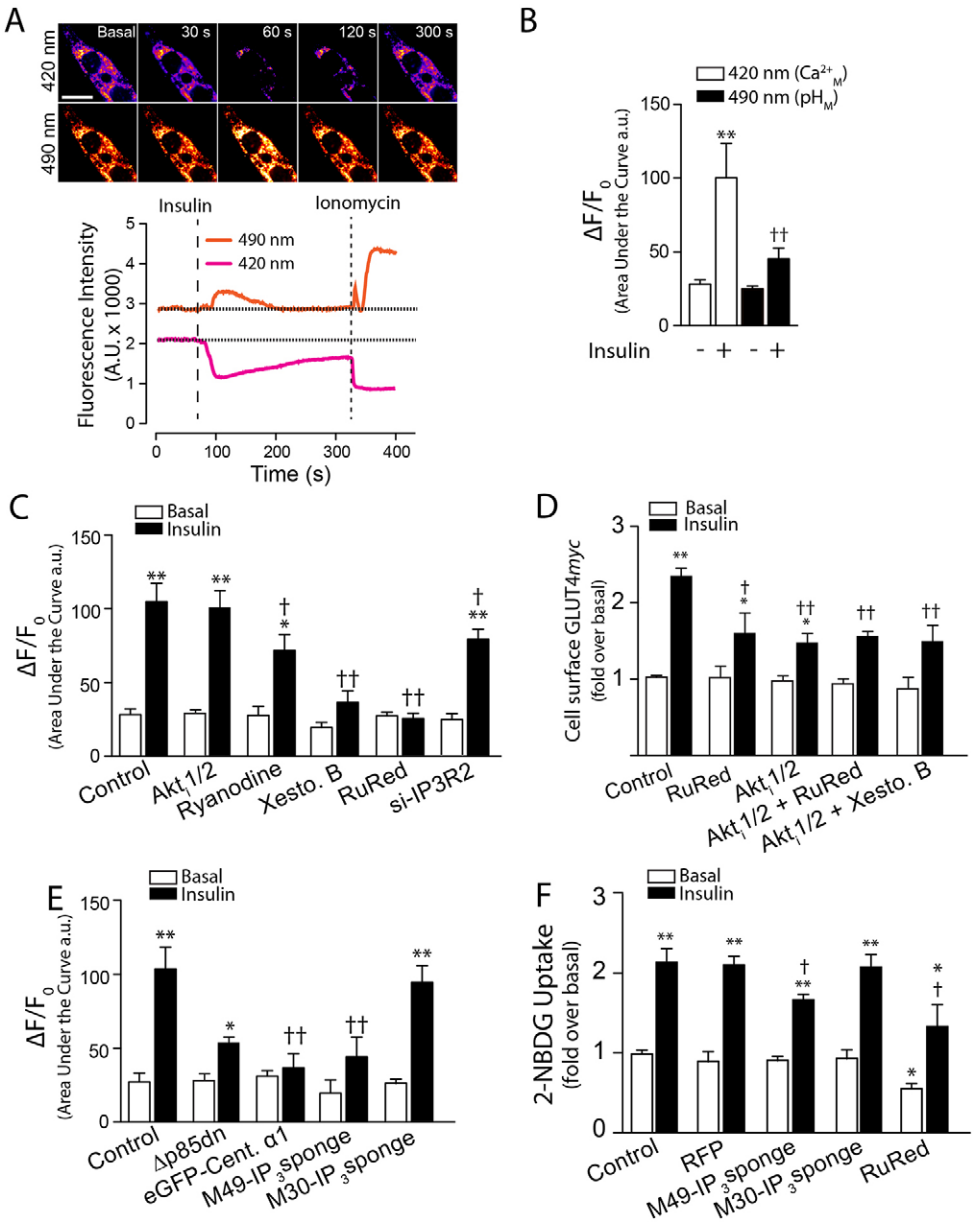

Fig. 6. Insulin induces IP3R-dependent mitochondrial Ca^{2+} and pH increases in L6GLUT4myc myotubes, which enhance GLUT4 translocation to the cell surface. (A) Representative fluorescence images recorded before and at different times after insulin addition. Myotubes transfected with mito-PeriCaM for 4 h were maintained for 24 h before adding 100 nM insulin; mito-PeriCaM fluorescence was determined at 525 nm following excitation at 420 nm or 490 nm. The lower panel illustrates the respective changes in fluorescence versus time. Cells were treated with 100 nM insulin (vertical long-dashed line) and then with 1 μM ionomycin (a Ca^{2+} ionophore), as a positive control (vertical short-dashed line). (B) The mean area under the curves, such as those shown in A, illustrating the time-dependent Ca^{2+} and pH changes (excitation at 420 nm or 490 nm, respectively) caused by addition of 100 nM insulin was calculated. (C) The mean area under the curves illustrating insulin-induced mitochondrial Ca^{2+}changes with time, was calculated from fluorescence traces recorded from control myotubes or from myotubes under the following conditions. Myotubes were pre-incubated with 10 μM $Akt_i1/2$ (an Akt inhibitor) for 30 min, 50 μM ryanodine (an ryanodine receptor inhibitor) for 3 h, 5 μM Xestospongin B (an IP3R inhibitor) for 30 min, 5 μM Ruthenium Red (a mitochondrial Ca^{2+} uniporter inhibitor) for 30 min; records were obtained also from myotubes transfected with IP3R2 siRNA. (D) Cell surface GLUT4myc levels, evaluated before or 20 min after 100 nM insulin addition, were determined in control myotubes and in myotubes pre-incubated as follows: 5 μM Ruthenium Red for 30 min, 10 μM $Akt_i1/2$ for 30 min, 10 μM $Akt_i1/2$ plus 5 μM RuRed for 30 min, or 10 μM $Akt_i1/2$ plus 5 μM Xestospongin B for 30 min. The effect of Xestospongin B alone is shown in Fig. 5C. (E) Mean area under the curves, illustrating insulin-induced mitochondrial Ca^{2+} changes with time. Mean areas were calculated from fluorescence traces recorded in control primary myotubes transfected with mito-PeriCaM or primary myotubes that after four days of differentiation were co-transfected with mito-PeriCaM plus Δp85dn (competitive inhibitor of regulatory subunit of PI3K), eGFP-tagged centaurin α1 (eGFP-Cent. α1, a PIP_3 sequester), M49-IP3 (active IP_3) sponge or M30-IP_3 (inactive IP_3 sponge). (F) Basal and insulin-induced 2-NBDG uptake was determined in primary myotubes transfected with plasmid encode RFP (red fluorescence protein), M49-IP3 sponge or M30-IP3 sponge (for further details, see the Materials and Methods). Results in B–F are mean±s.d. *$P<0.01$, **$P<0.001$ compared with basal; †$P<0.01$, ††$P<0.001$ compared with insulin-stimulated cells (one-way ANOVA followed by Tukey post-hoc test).

Journal of Cell Science (2014) 127, 1911–1923 doi:10.1242/jcs.138982

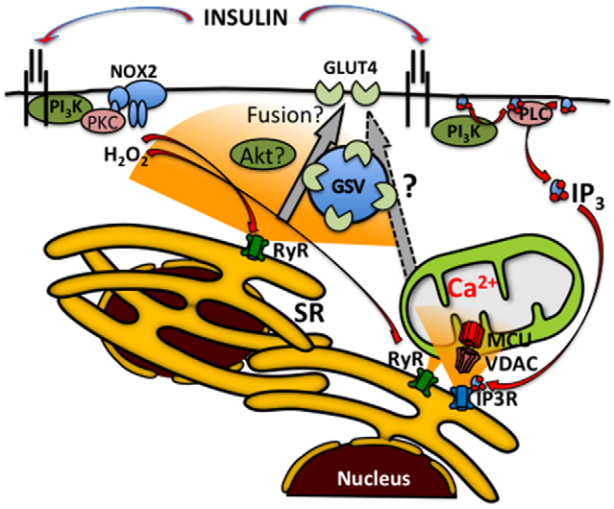

Fig. 7. Proposed model of Ca^{2+}-dependent glucose transport. Insulin-dependent GLUT4 translocation to the cell surface requires a complex mechanism involving Ca^{2+} release through both RyR and IP3R intracellular Ca^{2+} channels, which coordinately regulate insulin-induced stimulation of glucose transport. Insulin-mediated PI3K activation is common to both pathways. In one branch, insulin activates the NADPH oxidase NOX2 isoform through PKC-dependent stimulation, enhancing local ROS production (superoxide anion) that rapidly dismutates to H_2O_2, resulting in modification of RyR1 reactive cysteine residues. The ensuing Ca^{2+} release provides the Ca^{2+} signals required for GLUT4 translocation. In the parallel branch, insulin promotes IP_3 generation by PLC, which activates IP3R, causing local Ca^{2+} release and increasing mitochondrial Ca^{2+} uptake. This novel retrograde signal from mitochondria appears also to be involved in the regulation of GLUT4 translocation.

translocation (Rudich et al., 1998) and Akt and Rac1 activation (JeBailey et al., 2007). This is consistent with oxidative stress as a contributor factor to insulin resistance. Indeed, obese mice have a higher intracellular oxidative environment (Anderson et al., 2009) that could produce a decrease in glucose uptake, such as that presented in Fig. 1, at high H_2O_2 concentration.

The participation of NOX2 in insulin signaling has begun to emerge in a number of cellular systems. We previously reported that NOX2 activation mediates insulin-dependent Ca^{2+} release in primary myotubes (Espinosa et al., 2009); this study suggested that PKC participates in NOX2 activation, and it is known PKC promotes NOX2 activation in other systems (Gupte et al., 2009). In the present work, we confirmed the participation of PKC in insulin signaling. In fact, PKC inhibitors completely prevented insulin-induced H_2O_2 production, whereas PKC activation with PMA induced GLUT4 translocation. The fact that the stimulation produced by PMA was higher than that produced by insulin suggests that several different PKC isoforms participate in this process, not all of them sensitive to insulin signaling.

We further describe a specific role of insulin-dependent H_2O_2 production on RyR1 redox state. Sulfhydryl reagents modify selective RyR1 cysteine residues known as the 'hyper-reactive' cysteine residues (Zable et al., 1997). Modification of these hyper-reactive cysteine residues increases the open probability of RyR1 single channels (Marengo et al., 1998) and enhances RyR1-mediated Ca^{2+} release (Hidalgo et al., 2006). These hyper-reactive cysteine residues on RyR1 are targets for disulfide cross-linking, *S*-nitrosylation and/or *S*-glutathionylation (Aracena-Parks et al., 2006). In particular, a selective decrease in RyR1 channel inhibition by Mg^{2+} underlies the increased RyR1 activity induced by *S*-glutathionylation (Aracena et al., 2003). Protein modifications by *S*-glutathionylation have been implicated in the regulation of gene expression, cell signaling, ion channels, energy metabolism, mitochondria function, cell death and survival, cytoskeleton, folding and degradation (Pastore and Piemonte, 2012).

Based on those findings, it became important to assess the potential contribution of Ca^{2+} to downstream insulin action. Indeed, there are reports that GLUT4 exocytosis requires intracellular Ca^{2+} in adipocytes, allowing activation of Akt (Whitehead et al., 2001) and CDP138, a Ca^{2+}-dependent protein downstream of Akt (Xie et al., 2011). In skeletal muscle, however, direct evidence showing intracellular Ca^{2+}-dependent GLUT4 translocation was missing, although results have suggested that it occurs (Lanner et al., 2006; Wijesekara et al., 2006), and localized, sub-membrane changes in Ca^{2+} levels have been reported in response to the hormone (Bruton et al., 1999).

Here, we show that RyR1-mediated Ca^{2+} release, presumably through enhanced RyR1 *S*-glutathionylation, contributes solely to the cytoplasmic Ca^{2+} increase produced by insulin, which promotes insulin-induced GLUT4 translocation to the cell surface. Given that NOX2-dependent ROS generation leading to RyR1 *S*-glutathionylation and activation occurs in the skeletal muscle T-tubule membranes (Hidalgo et al., 2006), and GLUT4 preferentially inserts into the T-tubules in response to insulin (Marette et al., 1992), we speculate that short-term insulin-mediated cytoplasmic Ca^{2+} spikes near the T-tubule membrane allow vesicles containing the GLUT4 transporter to fuse into the T-tubule muscle membranes.

The IP3R–mitochondria branch

Intriguingly, we found that insulin also stimulates IP_3 production in myotubes, raising the question as to whether this intracellular mediator might also contribute to insulin-induced GLUT4 translocation. The observed reduction in GLUT4 translocation brought about by strategies designed to inhibit IP3R or dampen IP_3 levels support this prediction (Figs 5 and 6). Inhibition of RyR1 abolished the insulin-dependent Ca^{2+} spikes, indicating that IP3R-mediated Ca^{2+} release does not make a substantial contribution to the global cytoplasmic Ca^{2+} increase induced by insulin. Instead, our results show significant increases in mitochondrial Ca^{2+} originating from insulin-stimulated IP3R-mediated Ca^{2+} release, suggesting that mitochondria rapidly buffer the local Ca^{2+} changes produced by this pathway. We have not explored, however, whether H_2O_2 affects IP_3-dependent mitochondrial Ca^{2+} signals; this interesting possibility should be the subject of future studies. In addition, the impact of the IP3R–mitochondrial shunt might contribute to maintenance of mitochondrial function, adding to the overall anabolic function of insulin. It is interesting to note that incubation with ryanodine also has a partial effect on insulin-dependent mitochondria Ca^{2+} uptake (Fig. 6C); this can be interpreted in terms of a modulation of IP3Rs by Ca^{2+} coming from RyR, or a direct Ca^{2+} transfer from RyR to the mitochondria.

In conclusion, we find that insulin-activated NOX2 leads to *S*-glutathionylation and consequent activation of RyR1 that, in conjunction with activation of IP3R, contribute to insulin-dependent GLUT4 translocation. Future work should examine whether the transient increase in cytoplasmic Ca^{2+} potentiates elements in the canonical insulin signaling pathway constituted by PI3K and Akt and/or whether it directly promotes vesicle fusion with the surface membrane.

Journal of Cell Science (2014) 127, 1911–1923 doi:10.1242/jcs.138982

MATERIALS AND METHODS

Reagents

Penicillin-streptomycin and amphotericin B were obtained from Sigma-Aldrich. Dulbecco's modified Eagle's medium-F12, αMEM, bovine serum and fetal bovine serum (FBS) were from Invitrogen. Collagenase type II was from Worthington Biochemical Corp. Mini protease inhibitors were from Roche Applied Science. Secondary horseradish-peroxidase-conjugated anti-rabbit and anti-mouse Ig antibodies were from Pierce Biotechnology. Enhanced chemiluminescence reagents were from Amersham Pharmacia Biotech (Amersham, UK). Polyvinylidenedifluoride (PVDF) membranes were from Millipore. All other reagents were obtained from Sigma, Merck (Darmstadt, Germany) or Invitrogen. 2-NBDG and anti-rabbit or anti-mouse conjugated to Alexa Fluor 488 or 546 were from Molecular Probes. LY-294002 and Akt inhibitor VIII were from Calbiochem. Anti-Myc antibodies used were both polyclonal (Sigma-Aldrich) or monoclonal (sc40 clone, Santa Cruz Biotechnology). siRNA against p47phox was from Santa Cruz Biotechnology, siRNA against IP3R2 and Dharmafect was from Thermo Scientific.

Animals

Newborn rats were bred in the Animal Breeding Facility, Faculty of Medicine, Universidad de Chile (Santiago, Chile). Studies were approved by the Institutional Bioethical Committee, Faculty of Medicine, Universidad de Chile, in accordance with the 'Guide for the Care and Use of Laboratory Animals' (Bayne, 1996).

Cell cultures

Primary cultures of skeletal muscle cells were prepared from Sprague-Dawley neonatal rats as previously reported (Jaimovich et al., 2000). Six- to seven-day-old cultures were employed for the experiments. L6 muscle cells stable expressing GLUT4 with an exofacial Myc epitope (L6-GLUT4myc) were cultured as described previously (Wang et al., 1998).

Protein immunodetection

Western blot analysis was performed as previously reported (Contreras-Ferrat et al., 2010). The following primary antibodies and dilutions were used: anti-β-actin (1:3000 Cell Signaling) and anti-IP3R2 (1:2000; ABR, PA1-904). After scanning the films, densitometry analysis of the bands was performed with the Image J program (NIH, Bethesda, MD, USA).

^{3}H-2DG uptake

Myotubes were pre-incubated with inhibitors for 30 min and with insulin for 20 min in presence of each inhibitor. Glucose uptake was measured using 10 µM [^{3}H]2-deoxyglucose (^{3}H-2DG). To quantify ^{3}H-2DG uptake (0.1 µCi/well), myotubes were grown on 12-well plates (10^{6} cells per well) and treated with insulin in different conditions as detailed in the text. After stimulation, cells were washed with cold HEPES buffer solution and were later incubated with ^{3}H-2DG for 10 min on ice. Cold glucose solution (30 mM) was added to stop ^{3}H-2DG uptake. Cells were washed with 30 mM HEPES/glucose buffer and incubated with 0.05 M NaOH. Radioactivity was measured by liquid scintillation counting. Glucose uptake was expressed as fold over basal.

Intracellular Ca^{2+} measurements

Images were collected for 10 min using laser scanning confocal microscope in the frame-by-frame mode as previously reported (Contreras-Ferrat et al., 2010). L6 myotubes were preloaded with Fluo4 am (5 µM) at 37° for 30 min in Krebs Ringer buffer and stimulus were added to the microscopy chamber as indicated by arrows. BAPTA-AM (30 µM) was pre-incubated together with Fluo3 am whereas ryanodine (50 µM) was pre-incubated during 3 h. The dashed line in Fig. 3 represents medium replacement from Ca^{2+}-containing to Ca^{2+}-free conditions. Data were analyzed using ImageJ software.

Single-cell fluorescent hexose uptake assay

Analysis uptake of 2-NBDG was performed as previously reported (Osorio-Fuentealba et al., 2012). Approximately 100 cells in each condition were analyzed in different myotube cultures. The ImageJ software (NIH, Bethesda, MD, USA) was used to quantify 2-NBDG uptake in stimulated and non-stimulated cells. Glucose uptake is expressed as fold over basal (non-stimulated cells).

Recombinant adenoviruses

Adenovirus for catalase (AdCat) (Lam et al., 1999), cytosolic superoxide dismutase 1 (AdSOD1) (Zwacka et al., 1998) and empty construct (AdEmpty) were used to transduce myotubes at a multiplicity of infection (MOI) equivalent to 10,000 adenoviral particles per myotube for 24 h. Transduction efficiency was over 95% as monitored with adenovirus. Myotubes were infected with adenoviral vectors at a multiplicity of infection (MOI) of 1000 at least 24 h before use.

Quantification of cell surface GLUT4myc

A previously described assay was used (Wang et al., 1998). Briefly, cells grown in 12- or 24-well plates and serum starved for 3 h were treated with 100 nM insulin. The reaction was stopped with 0.25 ml per well of 3 M HCl. Supernatants were collected and absorbance was measured at 492 nm. To determine the level of GLUT4myc stain in single cells, the experiments were performed as previously described by (Wang et al., 1999).

Plasmid transfection, immunofluorescence microscopy and intracellular H_2O_2 detection

Myotubes were transfected with 3 µg of NES-PV-DsRed, Hyper-cyto, M49-IP3 sponge, M30-IP3 sponge, Δp85dn, eGFP-tagged centaurin α1, RFP or mitoPeriCaM using 6 µL/ml Lipofectamine^{TM} 2000 (Invitrogen). Transfection efficiency was over 80%. Plasmid-treated cells were incubated with transfection mixture for 4 h in penicillin-streptomycin and FBS-free OPTI-MEM (Invitrogen) medium. Myotubes were incubated in αMEM or F12-DMEM (1:1) for 24 h, and stimulated and processed according to each experimental protocol. The level of cell surface GLUT4myc was determined as described previously (Contreras-Ferrat et al., 2010; Wang et al., 1999). 1 µm *z*-stack images were acquired by laser scanning confocal microscope (CarlZeissPascal5, 63× NA1.4 objectives, Oberkochen, Germany). All materials used were free of detergent to avoid cell permeabilization. For GLUT4myc cell surface detection, >20 cells were analyzed in each condition from four different cultures. The HyPer-cytoplasmid has cpYFP inserted into OxyR-RD and displays submicromolar affinity for H_2O_2 (Belousov et al., 2006). Addition of 100 µM H_2O_2 to myotubes 24 h post-transfection caused a rapid and transient increase in intracellular HyPer-cyto fluorescence (ratio 490:420 nm).

Determination of intracellular IP_3 production

Control or experimental L6-GLUT4myc myotubes were quickly frozen in liquid nitrogen and were homogenized in 20 mM Tris-HCl pH 7.5, 2 mM EDTA, 150 mM NaCl and 0.5% Triton X-100. Determinations of IP_3 production were performed with an IP_3 ELISA Kit (Cusabio Biotech) following the manufacturer's instructions.

Statistical analysis

Data from at least four independent experiments are expressed as mean±s.d. The significance of difference among treatments was evaluated using a Student's *t*-test for unpaired data or by analysis of variance followed by Tukey post-hoc test. $P<0.01$ was considered statistically significant.

Competing interests

The authors declare no competing interests.

Author contributions

A.C.F. proposed the original idea; A.E. and E.J. contributed to the experimental design; A.C.F., P.L.I., C.V. performed Ca^{2+} measurements, GLUT4myc translocations and transfections; A.C.F., C.O.F. performed 2-NBDG uptake; A.C.F., M.A.C. and E.J. performed P.L.A. imaging and analysis; A.C.F., A.E., S.L., A.K., C.H. and E.J. analyzed results and wrote the manuscript.

Funding

This work was supported by FONDECYT [grant numbers 3110170 and 11130267 to A.C.-F., 3110105 to P.L., ACT1111 to E.J., S.L., A.E., 1100052 and BNI

P-09-015 to C.H.]; and Canadian Institutes of Health Research [grant number MT 7307 to A.K.]. C.V. and M.A-C. hold PhD fellowships from CONICYT, Chile.

Funding

This work was supported by FONDECYT [grant numbers 3110170 and 11130267 to A.C.-F., 3110105 to P.L., ACT1111 to E.J., S.L., A.E., 1100052 and BNI P-09-015 to C.H.]; and Canadian Institutes of Health Research [grant number MT 7307 to A.K.]. C.V. and M.A-C. hold PhD fellowships from CONICYT, Chile.

Supplementary material

Supplementary material available online at
http://jcs.biologists.org/lookup/suppl/doi:10.1242/jcs.138982/-/DC1

References

Anderson, E. J., Lustig, M. E., Boyle, K. E., Woodlief, T. L., Kane, D. A., Lin, C. T., Price, J. W., 3rd, Kang, L., Rabinovitch, P. S., Szeto, H. H. et al. (2009). Mitochondrial H2O2 emission and cellular redox state link excess fat intake to insulin resistance in both rodents and humans. *J. Clin. Invest.* **119**, 573-581.

Aracena, P., Sánchez, G., Donoso, P., Hamilton, S. L. and Hidalgo, C. (2003). S-glutathionylation decreases Mg2+ inhibition and S-nitrosylation enhances Ca2+ activation of RyR1 channels. *J. Biol. Chem.* **278**, 42927-42935.

Aracena-Parks, P., Goonasekera, S. A., Gilman, C. P., Dirksen, R. T., Hidalgo, C. and Hamilton, S. L. (2006). Identification of cysteines involved in S-nitrosylation, S-glutathionylation, and oxidation to disulfides in ryanodine receptor type 1. *J. Biol. Chem.* **281**, 40354-40368.

Bannister, R. A. (2013). Dantrolene-induced inhibition of skeletal L-type Ca2+ current requires RyR1 expression. *Biomed Res. Int.* **2013**, 390493.

Barreiro, E. and Hussain, S. N. (2010). Protein carbonylation in skeletal muscles: impact on function. *Antioxid. Redox Signal.* **12**, 417-429.

Bashan, N., Kovsan, J., Kachko, I., Ovadia, H. and Rudich, A. (2009). Positive and negative regulation of insulin signaling by reactive oxygen and nitrogen species. *Physiol. Rev.* **89**, 27-71.

Bayne, K.; American Physiological Society (1996). Revised guide for the care and use of laboratory animals available. *Physiologist* **39**, 199, 208-211.

Bedard, K. and Krause, K. H. (2007). The NOX family of ROS-generating NADPH oxidases: physiology and pathophysiology. *Physiol. Rev.* **87**, 245-313.

Belousov, V. V., Fradkov, A. F., Lukyanov, K. A., Staroverov, D. B., Shakhbazov, K. S., Terskikh, A. V. and Lukyanov, S. (2006). Genetically encoded fluorescent indicator for intracellular hydrogen peroxide. *Nat. Methods* **3**, 281-286.

Bouallegue, A., Pandey, N. R. and Srivastava, A. K. (2009). CaMKII knockdown attenuates H2O2-induced phosphorylation of ERK1/2, PKB/Akt, and IGF-1R in vascular smooth muscle cells. *Free Radic. Biol. Med.* **47**, 858-866.

Bruton, J. D., Katz, A. and Westerblad, H. (1999). Insulin increases near-membrane but not global Ca2+ in isolated skeletal muscle. *Proc. Natl. Acad. Sci. USA* **96**, 3281-3286.

Contreras-Ferrat, A. E., Toro, B., Bravo, R., Parra, V., Vásquez, C., Ibarra, C., Mears, D., Chiong, M., Jaimovich, E., Klip, A. et al. (2010). An inositol 1,4,5-triphosphate (IP3)-IP3 receptor pathway is required for insulin-stimulated glucose transporter 4 translocation and glucose uptake in cardiomyocytes. *Endocrinology* **151**, 4665-4677.

Donoso, P., Aracena, P. and Hidalgo, C. (2000). Sulfhydryl oxidation overrides Mg(2+) inhibition of calcium-induced calcium release in skeletal muscle triads. *Biophys. J.* **79**, 279-286.

Eltit, J. M., Yang, T., Li, H., Molinski, T. F., Pessah, I. N., Allen, P. D. and Lopez, J. R. (2010). RyR1-mediated Ca2+ leak and Ca2+ entry determine resting intracellular Ca2+ in skeletal myotubes. *J. Biol. Chem.* **285**, 13781-13787.

Espinosa, A., Estrada, M. and Jaimovich, E. (2004). IGF-I and insulin induce different intracellular calcium signals in skeletal muscle cells. *J. Endocrinol.* **182**, 339-352.

Espinosa, A., García, A., Härtel, S., Hidalgo, C. and Jaimovich, E. (2009). NADPH oxidase and hydrogen peroxide mediate insulin-induced calcium increase in skeletal muscle cells. *J. Biol. Chem.* **284**, 2568-2575.

Fonteriz, R. I., de la Fuente, S., Moreno, A., Lobatón, C. D., Montero, M. and Alvarez, J. (2010). Monitoring mitochondrial [Ca(2+)] dynamics with rhod-2, ratiometric pericam and aequorin. *Cell Calcium* **48**, 61-69.

Forman, H. J., Maiorino, M. and Ursini, F. (2010). Signaling functions of reactive oxygen species. *Biochemistry* **49**, 835-842.

Foskett, J. K., White, C., Cheung, K. H. and Mak, D. O. (2007). Inositol trisphosphate receptor Ca2+ release channels. *Physiol. Rev.* **87**, 593-658.

Gupte, S. A., Kaminski, P. M., George, S., Kouznestova, L., Olson, S. C., Mathew, R., Hintze, T. H. and Wolin, M. S. (2009). Peroxide generation by p47phox-Src activation of Nox2 has a key role in protein kinase C-induced arterial smooth muscle contraction. *Am. J. Physiol.* **296**, H1048-H1057.

Hidalgo, C. and Donoso, P. (2008). Crosstalk between calcium and redox signaling: from molecular mechanisms to health implications. *Antioxid. Redox Signal.* **10**, 1275-1312.

Hidalgo, C., Bull, R., Behrens, M. I. and Donoso, P. (2004). Redox regulation of RyR-mediated Ca2+ release in muscle and neurons. *Biol. Res.* **37**, 539-552.

Hidalgo, C., Sánchez, G., Barrientos, G. and Aracena-Parks, P. (2006). A transverse tubule NADPH oxidase activity stimulates calcium release from isolated triads via ryanodine receptor type 1 S -glutathionylation. *J. Biol. Chem.* **281**, 26473-26482.

Horie, T., Ono, K., Nagao, K., Nishi, H., Kinoshita, M., Kawamura, T., Wada, H., Shimatsu, A., Kita, T. and Hasegawa, K. (2008). Oxidative stress induces GLUT4 translocation by activation of PI3-K/Akt and dual AMPK kinase in cardiac myocytes. *J. Cell. Physiol.* **215**, 733-742.

Ishikura, S. and Klip, A. (2008). Muscle cells engage Rab8A and myosin Vb in insulin-dependent GLUT4 translocation. *Am. J. Physiol.* **295**, C1016-C1025.

Jaimovich, E. and Carrasco, M. A. (2002). IP3 dependent Ca2+ signals in muscle cells are involved in regulation of gene expression. *Biol. Res.* **35**, 195-202.

Jaimovich, E., Reyes, R., Liberona, J. L. and Powell, J. A. (2000). IP(3) receptors, IP(3) transients, and nucleus-associated Ca(2+) signals in cultured skeletal muscle. *Am. J. Physiol.* **278**, C998-C1010.

Javeshghani, D., Magder, S. A., Barreiro, E., Quinn, M. T. and Hussain, S. N. (2002). Molecular characterization of a superoxide-generating NAD(P)H oxidase in the ventilatory muscles. *Am. J. Respir. Crit. Care Med.* **165**, 412-418.

JeBailey, L., Wanono, O., Niu, W., Roessler, J., Rudich, A. and Klip, A. (2007). Ceramide- and oxidant-induced insulin resistance involve loss of insulin-dependent Rac-activation and actin remodeling in muscle cells. *Diabetes* **56**, 394-403.

Lam, E. W., Zwacka, R., Seftor, E. A., Nieva, D. R., Davidson, B. L., Engelhardt, J. F., Hendrix, M. J. and Oberley, L. W. (1999). Effects of antioxidant enzyme overexpression on the invasive phenotype of hamster cheek pouch carcinoma cells. *Free Radic. Biol. Med.* **27**, 572-579.

Lanner, J. T., Katz, A., Tavi, P., Sandström, M. E., Zhang, S. J., Wretman, C., James, S., Fauconnier, J., Lännergren, J., Bruton, J. D. et al. (2006). The role of Ca2+ influx for insulin-mediated glucose uptake in skeletal muscle. *Diabetes* **55**, 2077-2083.

Lanner, J. T., Bruton, J. D., Assefaw-Redda, Y., Andronache, Z., Zhang, S. J., Severa, D., Zhang, Z. B., Melzer, W., Zhang, S. L., Katz, A. et al. (2009). Knockdown of TRPC3 with siRNA coupled to carbon nanotubes results in decreased insulin-mediated glucose uptake in adult skeletal muscle cells. *FASEB J.* **23**, 1728-1738.

Li, Y., Wang, P., Xu, J. and Desir, G. V. (2006). Voltage-gated potassium channel Kv1.3 regulates GLUT4 trafficking to the plasma membrane via a Ca2+ -dependent mechanism. *Am. J. Physiol.* **290**, C345-C351.

Liberona, J. L., Cárdenas, J. C., Reyes, R., Hidalgo, J., Molgó, J. and Jaimovich, E. (2008). Sodium-dependent action potentials induced by brevetoxin-3 trigger both IP3 increase and intracellular Ca2+ release in rat skeletal myotubes. *Cell Calcium* **44**, 289-297.

Liu, L. Z., Zhao, H. L., Zuo, J., Ho, S. K., Chan, J. C., Meng, Y., Fang, F. D. and Tong, P. C. (2006). Protein kinase Czeta mediates insulin-induced glucose transport through actin remodeling in L6 muscle cells. *Mol. Biol. Cell* **17**, 2322-2330.

Loh, K., Deng, H., Fukushima, A., Cai, X., Boivin, B., Galic, S., Bruce, C., Shields, B. J., Skiba, B., Ooms, L. M. et al. (2009). Reactive oxygen species enhance insulin sensitivity. *Cell Metab.* **10**, 260-272.

Maghzal, G. J., Krause, K. H., Stocker, R. and Jaquet, V. (2012). Detection of reactive oxygen species derived from the family of NOX NADPH oxidases. *Free Radic. Biol. Med.* **53**, 1903-1918.

Mahadev, K., Wu, X., Zilbering, A., Zhu, L., Lawrence, J. T. and Goldstein, B. J. (2001). Hydrogen peroxide generated during cellular insulin stimulation is integral to activation of the distal insulin signaling cascade in 3T3-L1 adipocytes. *J. Biol. Chem.* **276**, 48662-48669.

Marengo, J. J., Hidalgo, C. and Bull, R. (1998). Sulfhydryl oxidation modifies the calcium dependence of ryanodine-sensitive calcium channels of excitable cells. *Biophys. J.* **74**, 1263-1277.

Marette, A., Burdett, E., Douen, A., Vranic, M. and Klip, A. (1992). Insulin induces the translocation of GLUT4 from a unique intracellular organelle to transverse tubules in rat skeletal muscle. *Diabetes* **41**, 1562-1569.

Osorio-Fuentealba, C., Contreras-Ferrat, A. E., Altamirano, F., Espinosa, A., Li, Q., Niu, W., Lavandero, S., Klip, A. and Jaimovich, E. (2012). Electrical stimuli release ATP to increase GLUT4 translocation and glucose uptake via PI3Kgamma-Akt-AS160 in skeletal muscle cells. *Diabetes*. **62**, 1519-1526.

Pacher, P., Sharma, K., Csordás, G., Zhu, Y. and Hajnóczky, G. (2008). Uncoupling of ER-mitochondrial calcium communication by transforming growth factor-beta. *Am. J. Physiol.* **295**, F1303-F1312.

Pastore, A. and Piemonte, F. (2012). S-Glutathionylation signaling in cell biology: progress and prospects. *Eur. J. Pharm. Sci.* **46**, 279-292.

Paulsen, C. E. and Carroll, K. S. (2010). Orchestrating redox signaling networks through regulatory cysteine switches. *ACS Chem. Biol.* **5**, 47-62.

Powell, D. J., Hajduch, E., Kular, G. and Hundal, H. S. (2003). Ceramide disables 3-phosphoinositide binding to the pleckstrin homology domain of protein kinase B (PKB)/Akt by a PKCzeta-dependent mechanism. *Mol. Cell. Biol.* **23**, 7794-7808.

Protasi, F., Paolini, C., Nakai, J., Beam, K. G., Franzini-Armstrong, C. and Allen, P. D. (2002). Multiple regions of RyR1 mediate functional and structural interactions with alpha(1S)-dihydropyridine receptors in skeletal muscle. *Biophys. J.* **83**, 3230-3244.

Rudich, A., Tirosh, A., Potashnik, R., Hemi, R., Kanety, H. and Bashan, N. (1998). Prolonged oxidative stress impairs insulin-induced GLUT4 translocation in 3T3-L1 adipocytes. *Diabetes* **47**, 1562-1569.

San José, G., Bidegain, J., Robador, P. A., Díez, J., Fortuño, A. and Zalba, G. (2009). Insulin-induced NADPH oxidase activation promotes proliferation and

matrix metalloproteinase activation in monocytes/macrophages. *Free Radic. Biol. Med.* **46**, 1058-1067.

Söderberg, O., Gullberg, M., Jarvius, M., Ridderstråle, K., Leuchowius, K. J., Jarvius, J., Wester, K., Hydbring, P., Bahram, F., Larsson, L. G. et al. (2006). Direct observation of individual endogenous protein complexes in situ by proximity ligation. *Nat. Methods* **3**, 995-1000.

Stretton, C., Evans, A. and Hundal, H. S. (2010). Cellular depletion of atypical PKClambda is associated with enhanced insulin sensitivity and glucose uptake in L6 rat skeletal muscle cells. *Am. J. Physiol.* **299**, E402-E412.

Wang, Q., Khayat, Z., Kishi, K., Ebina, Y. and Klip, A. (1998). GLUT4 translocation by insulin in intact muscle cells: detection by a fast and quantitative assay. *FEBS Lett.* **427**, 193-197.

Wang, Q., Somwar, R., Bilan, P. J., Liu, Z., Jin, J., Woodgett, J. R. and Klip, A. (1999). Protein kinase B/Akt participates in GLUT4 translocation by insulin in L6 myoblasts. *Mol. Cell. Biol.* **19**, 4008-4018.

Wei, Y., Sowers, J. R., Clark, S. E., Li, W., Ferrario, C. M. and Stump, C. S. (2008). Angiotensin II-induced skeletal muscle insulin resistance mediated by NF-kappaB activation via NADPH oxidase. *Am. J. Physiol.* **294**, E345-E351.

Whitehead, J. P., Molero, J. C., Clark, S., Martin, S., Meneilly, G. and James, D. E. (2001). The role of Ca2+ in insulin-stimulated glucose transport in 3T3-L1 cells. *J. Biol. Chem.* **276**, 27816-27824.

Wijesekara, N., Tung, A., Thong, F. and Klip, A. (2006). Muscle cell depolarization induces a gain in surface GLUT4 via reduced endocytosis independently of AMPK. *Am. J. Physiol.* **290**, E1276-E1286.

Wright, D. C., Geiger, P. C., Rheinheimer, M. J., Han, D. H. and Holloszy, J. O. (2004). Phorbol esters affect skeletal muscle glucose transport in a fiber type-specific manner. *Am. J. Physiol.* **287**, E305-E309.

Wright, D. C., Geiger, P. C., Holloszy, J. O. and Han, D. H. (2005). Contraction- and hypoxia-stimulated glucose transport is mediated by a Ca2+-dependent mechanism in slow-twitch rat soleus muscle. *Am. J. Physiol.* **288**, E1062-E1066.

Wright, V. P., Reiser, P. J. and Clanton, T. L. (2009). Redox modulation of global phosphatase activity and protein phosphorylation in intact skeletal muscle. *J. Physiol.* **587**, 5767-5781.

Xie, X., Gong, Z., Mansuy-Aubert, V., Zhou, Q. L., Tatulian, S. A., Sehrt, D., Gnad, F., Brill, L. M., Motamedchaboki, K., Chen, Y. et al. (2011). C2 domain-containing phosphoprotein CDP138 regulates GLUT4 insertion into the plasma membrane. *Cell Metab.* **14**, 378-389.

Zable, A. C., Favero, T. G. and Abramson, J. J. (1997). Glutathione modulates ryanodine receptor from skeletal muscle sarcoplasmic reticulum. Evidence for redox regulation of the Ca2+ release mechanism. *J. Biol. Chem.* **272**, 7069-7077.

Zaid, H., Antonescu, C. N., Randhawa, V. K. and Klip, A. (2008). Insulin action on glucose transporters through molecular switches, tracks and tethers. *Biochem. J.* **413**, 201-215.

Zwacka, R. M., Dudus, L., Epperly, M. W., Greenberger, J. S. and Engelhardt, J. F. (1998). Redox gene therapy protects human IB-3 lung epithelial cells against ionizing radiation-induced apoptosis. *Hum. Gene Ther.* **9**, 1381-1386.